The Formation Conditions of Chondrules and Chondrites

C. M. O'D. Alexander, *et al.*

Science **320**, 1617 (2008);
DOI: 10.1126/science.1156561

Science (print ISSN 0036-8075; online ISSN 1095-9203) is published weekly, except the last week in December, by the American Association for the Advancement of Science, 1200 New York Avenue NW, Washington, DC 20005.

from the source to the measurement (fig. S2). The result (purple dashed line in Fig. 4B) is compared with the intrinsic attosecond chirp (green solid line in Fig. 4B) calculated from a classical trajectory analysis (*23*, *24*). There is a notable discrepancy at the high-energy components of the wave packet, possibly because of quantum effects near cutoff. Nevertheless, the agreement with the attochirp resulting from short trajectories is stunning in the main part of the spectrum, where the S/N ratio is excellent. This agreement indicates the powerfulness of semiclassical modeling of strong-field interactions (*25*, *26*) and the negligible role of long trajectories in contributing to the XUV radiation in the far field (*27*).

In a similar way, the confinement of interaction between the ionizing field and the atom to a single wave cycle will permit accurate quantitative tests of theories of strong-field ionization. The sub-100-as XUV pulses emerging from the interaction with a flux greater than 10^{11} photons/s—along with their monocycle NIR driver wave—will push the resolution limit of attosecond spectroscopy to the atomic unit of time (~24 as) and allow for the real-time observation of electron correlations, by means of streaking (*6*), tunneling (*14*), or absorption (*28*) spectroscopy.

References and Notes

1. A. Baltuska *et al.*, *Nature* **421**, 611 (2003).
2. R. Kienberger *et al.*, *Nature* **427**, 817 (2004).
3. E. Goulielmakis *et al.*, *Science* **305**, 1267 (2004).
4. M. F. Kling *et al.*, *Science* **312**, 246 (2006).
5. G. Sansone *et al.*, *Science* **314**, 443 (2006).
6. A. L. Cavalieri *et al.*, *Nature* **449**, 1029 (2007).
7. E. Goulielmakis *et al.*, *Science* **317**, 769 (2007).
8. S. Svensson, B. Eriksson, N. Martensson, G. Wendin, U. J. Gelius, *J. Electron Spectrosc. Relat. Phenom.* **47**, 327 (1988).
9. S. X. Hu, L. A. Collins, *Phys. Rev. Lett.* **96**, 073004 (2006).
10. J. Breidbach, L. S. Cederbaum, *Phys. Rev. Lett.* **94**, 033901 (2005).
11. A. I. Kuleff, J. Breidbach, L. S. Cederbaum, *J. Chem. Phys.* **123**, 044111 (2005).
12. F. Remacle, R. D. Levine, *Proc. Natl. Acad. Sci. U.S.A.* **103**, 6793 (2006).
13. G. Yudin, M. Y. Ivanov, *Phys. Rev. A* **64**, 035401 (2001).
14. M. Uiberacker *et al.*, *Nature* **446**, 627 (2007).
15. T. Pfeifer *et al.*, *Phys. Rev. Lett.* **97**, 163901 (2006).
16. Y. Oishi *et al.*, *Opt. Express* **14**, 7230 (2006).
17. See supporting material on *Science* Online.
18. C. A. Haworth *et al.*, *Nature Phys.* **3**, 52 (2007).
19. A. L. Cavalieri *et al.*, *New J. Phys.* **9**, 242 (2007).
20. R. Trebino, D. J. Kane, *J. Opt. Soc. Am. A* **10**, 1101 (1993).
21. Y. Mairesse, F. Quéré, *Phys. Rev. A* **71**, 011401(R) (2005).
22. D. J. Kane, G. Rodriguez, A. J. Taylor, T. S. Clement, *J. Opt. Soc. Am. B* **14**, 935 (1997).
23. P. Salières *et al.*, *Science* **292**, 902 (2001).
24. V. S. Yakovlev, A. Scrinzi, *Phys. Rev. Lett.* **91**, 153901 (2003).
25. P. B. Corkum, *Phys. Rev. Lett.* **71**, 1994 (1993).
26. K. J. Schafer, B. Yang, L. F. DiMauro, K. C. Kulander, *Phys. Rev. Lett.* **70**, 1599 (1993).
27. R. López-Martens *et al.*, *Phys. Rev. Lett.* **94**, 033001 (2005).
28. Z.-H. Loh *et al.*, *Phys. Rev. Lett.* **98**, 143601 (2007).
29. K. Varjú *et al.*, *Laser Phys.* **15**, 888 (2005).

30. Supported by the Max Planck Society and the Deutsche Forschungsgemeinschaft Cluster of Excellence: Munich Centre for Advanced Photonics (www.munich-photonics.de). E.G. acknowledges a Marie-Curie fellowship (MEIF-CT-2005-02440) and a Marie-Curie Reintegration grant (MERG-CT-2007-208643). A.L.A. is supported by the NSF Extreme Ultraviolet Engineering Research Center. R.K. acknowledges support from the Sofia Kovalevskaya award of the Alexander von Humboldt Foundation.

Supporting Online Material

www.sciencemag.org/cgi/content/320/5883/1614/DC1
SOM Text
Figs. S1 to S4
References

17 March 2008; accepted 27 May 2008
10.1126/science.1157846

The Formation Conditions of Chondrules and Chondrites

C. M. O'D. Alexander,[1]* J. N. Grossman,[2] D. S. Ebel,[3] F. J. Ciesla[1]

Chondrules, which are roughly millimeter-sized silicate-rich spherules, dominate the most primitive meteorites, the chondrites. They formed as molten droplets and, judging from their abundances in chondrites, are the products of one of the most energetic processes that operated in the early inner solar system. The conditions and mechanism of chondrule formation remain poorly understood. Here we show that the abundance of the volatile element sodium remained relatively constant during chondrule formation. Prevention of the evaporation of sodium requires that chondrules formed in regions with much higher solid densities than predicted by known nebular concentration mechanisms. These regions would probably have been self-gravitating. Our model explains many other chemical characteristics of chondrules and also implies that chondrule and planetesimal formation were linked.

Chondrules make up ~20 to 80 volume % of most chondrites and formed at peak temperatures of ~1700 to 2100 K (*1*). Chondrules in the different chondrite groups have distinct physical and chemical properties (*2*), as well as distinct age ranges (*3*), indicating that they formed in relatively local environments via a process that operated at least periodically between ~1 and 4 million years after the formation of the solar system.

It was long thought that individual chondrules behaved as chemically closed systems during their formation, inheriting their compositions from their precursors (*4*, *5*). However, for likely cooling rates of 10 to 1000 K/hour (*1*) and at the low pressures (total pressure ≈ 10^{-6} to 10^{-3} bars) of the solar protoplanetary disk (nebula), experiments (*6*–*8*), natural analogs (*9*, *10*), and theoretical calculations (*11*, *12*) all show that there should be extensive evaporation of major and minor elements, in the order S > Na, K > Fe > Si > Mg.

Elemental fractionations in chondrules are generally a function of volatility (*4*, *5*). If evaporation in the nebula produced the alkali metal and Fe fractionations, the more volatile elements (such as S) should be entirely absent, which they are not. In addition, the fractionated elements should exhibit large and systematic isotopic fractionations, which they do not (*13*).

Here we demonstrate that chondrules did indeed behave as essentially closed systems during melting, at least for elements with volatilities less than or equal to that of Na. We also propose a means of resolving the apparent conflict between this result and experimental and theoretical expectations that chondrules should have suffered considerable evaporation during formation. Our conclusions have implications for mechanisms of dust concentration in the solar nebula, for chondrule formation, and for planetesimal formation.

Chondrules are dominated by olivine [$(Mg,Fe)_2SiO_4$], pyroxene [$(Mg,Fe,Ca)SiO_3$], Fe-Ni metal, and quenched silicate melt (glass). Many of the more volatile elements (such as Na) can diffuse rapidly, particularly in melts and glasses. Therefore, it is possible that volatiles were completely lost when chondrules melted, and reentered the chondrules during cooling or even after solidification. However, Na clinopyroxene/glass ratios show that the Na contents of the final chondrule melts (now glass) had approximately their observed, relatively high abundances at temperatures of ~1600 to 1200 K (*14*–*16*).

Calculations suggest that chondrule melts could have been stabilized in the nebula by substantially enriching solids (chondrule precursors or other dust) relative to gas (*11*, *12*). This also substantially increases the condensation temperatures of even highly volatile elements such as S (*11*, *12*). Even in solid-enriched systems, there is an initial phase of evaporation when a chondrule melts, but subsequent chondrule/gas re-equilibration would erase any isotopic fractionations (*12*). If the enrichment of solids is high, little evaporation may be needed to reach chondrule/gas equilibrium, and the behavior of volatile elements during cooling would resemble closed-system behavior. However, even at a high total pressure of 10^{-3} bars, with a solids enrichment of 1000 relative to the solar composition, all the Na would evaporate at near-liquidus temperatures, and substantial recondensation only begins well below 1600 K (*11*). Locally enriching chondrule-sized or smaller solids by 1000 times

[1]Department of Terrestrial Magnetism, Carnegie Institution of Washington, Washington, DC 20015, USA. [2]U.S. Geological Survey, Reston, VA 20192, USA. [3]American Museum of Natural History, New York, NY 10024, USA.

*To whom correspondence should be addressed. E-mail: alexande@dtm.ciw.edu

on substantial spatial scales would have been difficult to achieve in the nebula with known mechanisms (*17*), except perhaps if levels of turbulence were very low (*18*).

It is evident from the above that the behavior of Na during cooling can constrain the degree to which solids were enriched during chondrule formation. Olivine is the highest-temperature liquidus phase in chondrules and is predicted to crystallize throughout much of their supersolidus cooling (*11*). Olivine phenocrysts in chondrules are generally zoned in major and minor elements, demonstrating that olivine cores did not maintain equilibrium with the liquid during cooling. Na does partition into olivine, albeit at low levels. Therefore, if Na could be measured in them, olivine phenocrysts should record any changes in the Na content of their host chondrules as they crystallized.

We analyzed bulk, mineral, and glass compositions in 26 Semarkona (classified as a LL3.0) chondrules (Table 1) (*18*) with a range of types (IA-IAB and IIA-IIAB-IIB, where I = FeO-poor, II = FeO-rich, A = olivine-dominated, B = pyroxene-dominated, and AB = intermediate). In general, chondrule olivines exhibit pronounced normal zoning in major (Mg and Fe) and minor (Na, Cr, Mn, and Ca) elements that is consistent with expectations for crystallization from their bulk chondrule melts (*5*, *16*, *19*). Na can diffuse rapidly in some minerals and glasses at high temperature, but the fact that its zoning roughly parallels that of Cr, Mn, and Ca demonstrates its primary nature. In addition, the shapes of Na zoning profiles around Na- and Fe-poor relict olivine grains (unmelted precursors) (*20*, *21*) in type II chondrules are similar to or broader than those of Fe (*22*), suggesting that Na diffusion rates in these olivines were comparable to those of Fe. Except where grains are clearly relict, analyses of phenocrysts and microphenocrysts from the same chondrule fall on similar trends, but these trends commonly differ from chondrule to chondrule.

The simple observation of measurable Na in the cores of chondrule olivines (Fig. 1 and Table 1) (*18*) is contrary to predictions (Fig. 1), even in what has previously been considered a highly dust-enriched system (1000 times that of the solar composition) (*11*). To determine how much Na was present in the chondrule melts during olivine crystallization, it is necessary to know the Na olivine-melt distribution coefficient (K_D), measurements of which have yet to be published. However, clinopyroxene-glass partitioning demonstrates that the Na contents of the glass in the central regions of these chondrules were established before solidification (*14*–*16*). In olivine-normative chondrules, olivine was generally still on the liquidus at the onset of clinopyroxene crystallization [calculated with MELTS (*23*)]. Consequently, we can estimate the olivine-liquid K_D for Na at the end of crystallization for each chondrule as the ratio of the Na_2O contents of the last olivine to form (the most Na- and Fe-rich phenocryst rims and microphenocrysts) to that in the glass (rim K_Ds, Table 1). The rim K_Ds are fairly similar for all chondrules, implying no strong compositional dependence.

To determine whether bulk chondrule Na abundances were very different at liquidus

Table 1. The petrologic types and estimated liquidus temperatures of the Semarkona chondrules studied, as well as the Mg number and Na olivine-melt K_Ds of the first (core) and last (rim) olivines to crystallize.

Chondrule	Type	Liquidus* (°C)	Core† Mg no.	Rim† Mg no.	Core§ K_D	Rim‖ K_D	Density¶ (g/m^3)
C1	IIA	1680	0.898	0.699	0.0077(11)	0.0068(13)	17 to 311
C2	IIA	1652	0.888	0.796	0.0028(07)	0.0028(06)	12 to 194
C3	IIA	1658	0.898	0.716	0.0095(13)	0.0063(02)	14 to 251
C4	IIA	1702	0.905	0.771	0.0074(15)	0.0061(07)	33 to 476
C5	IIA	1646	0.792	0.722	0.015(02)	0.0053(09)	14 to 229
C6	IA‡#	1706	0.994	0.995	0.019(05)	0.0055(45)	91 to 2510
C7	IA	1716	0.996	0.994	0.0011(14)	0.0023(12)	51 to 1610
C8	IAB‡	1752	0.994	0.994	0.0066(44)	0.0025(12)	118 to 3090
C9	IAB‡	1770	0.993	0.993	0.025(13)	0.0081(40)	198 to 5750
C10	IIA	1642		0.791		0.0061(08)	11 to 194
C11	IA‡	1778	0.993	0.992	0.069(18)	0.0063(42)	388 to 9080
C13	IIAB	1582	0.846	0.647	0.0028(05)	0.0046(03)	3 to 60
C14	IIA	1672	0.909	0.675	0.0032(07)	0.0041(05)	16 to 260
C18	IIAB	1646	0.840	0.766	0.0031(06)	0.0020(02)	10 to 165
C19	IIAB	1630	0.936	0.888	0.0009(06)	0.0009(01)	6 to 117
C20	IIA	1718	0.923	0.795	0.0040(09)	0.0030(05)	32 to 526
C22	IIA	1678	0.910	0.688	0.0057(09)	0.0054(05)	15 to 273
C23	IIAB	1634	0.875	0.690	0.0014(06)	0.0031(04)	10 to 158
C27	IIAB	1674	0.875	0.780	0.0060(11)	0.0014(02)	14 to 259
C29	IIAB	1612	0.871	0.840	0.0009(05)	0.0003(01)	6 to 99
C31	IIAB	1630	0.849	0.696	0.0059(10)	0.0020(01)	7 to 128
C33	IIA#	1632	0.854	0.806	0.0024(06)	0.0027(01)	9 to 167
C34	IIAB	1554		0.738		0.0033(08)	2 to 43
C35	IIA	1580	0.835	0.745	0.0057(07)	0.0047(02)	4 to 72
C38	IIA	1704	0.866	0.813	0.0034(10)	0.0027(02)	30 to 534
C40	IIB	1622	0.858		0.0056(20)		6 to 139

*Liquidus temperatures were estimated with MELTS (*23*). †Mg number is the atomic Mg/(Mg+Fe) number of the olivine. ‡The alkali metals in the glasses of these chondrules are radially zoned. The core glass compositions were used for the rim K_Ds and to calculate the initial bulk compositions. §The errors are based only on the uncertainty of the Na measurements in the olivine cores and a nominal 10% error in the bulk compositions. ‖The errors are based only on uncertainties in the measured olivine and glass compositions. ¶Upper and lower density limits assume that 90% of the Na remained condensed. The lower limit assumes a vapor in equilibrium with a silicate melt only. The upper limit assumes a vapor in equilibrium with silicate and pure Fe-metal melts. #All chondrules have porphyritic textures, except C6 and C33, which are barred.

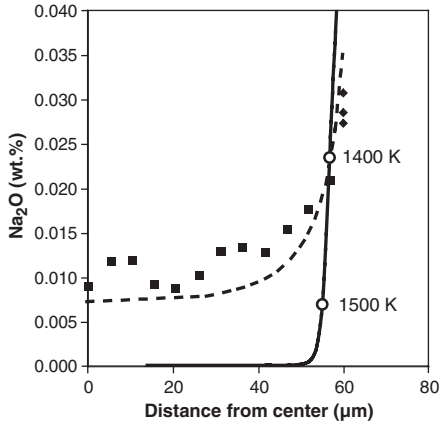

Fig. 1. Comparison of the Na_2O radial zonation in an olivine phenocryst (squares) from chondrule C3 with predictions (*18*) for closed-system crystallization (dashed line) and a chondrule forming in a region of the nebula with a total pressure of 10^{-3} bars that is enriched in solids relative to a solar gas by a factor of 1000 (solid line). wt %, weight %. The predictions assume an olivine-melt K_D of 0.0075 (Table 1). The diamond symbols represent microphenocrysts in the glass that probably most closely reflect the compositions of the last olivine to be in equilibrium with the glass.

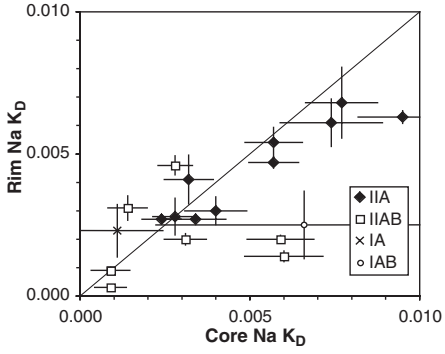

Fig. 2. The initial (core) and final (rim) olivine Na K_Ds for most of the Semarkona chondrules studied (Table 1). Four chondrules with large core K_Ds fall outside the figure.

temperatures, when olivine began to grow (~400 to 500 K above the clinopyroxene and final olivine crystallization temperatures), we calculated the apparent K_Ds for the cores of olivine grains. We did this for each chondrule, using their most Na- and Fe-poor core olivine compositions and their bulk Na content (core K_Ds, Table 1). Figure 2 compares the apparent core and rim K_Ds. Most chondrules fall close to the 1:1 line, as would be expected for closed-system behavior. The notable exceptions, which all fall well to the right of the 1:1 line and out of the figure, are the three type IAs and chondrule C5, which have very high core K_Ds. We suspect that this is because they contain unrecognized relatively Na-rich relict cores. The good correspondence between core and rim K_Ds for most chondrules, which cover several hundred degrees of cooling, suggests that (i) they do not have strong temperature or compositional dependences, and (ii) the Na contents of most chondrules did not vary dramatically during cooling. This inference is supported by the subparallel Na, Cr, Mn, and Ca zoning profiles in most olivine phenocrysts. Some chondrules do have core K_Ds that, for the quoted errors, are significantly lower than the rim K_Ds, which could be indicative of some Na gain by the melt during cooling, although the differences are still much less than predicted by the most solids-enriched model of (*11*).

There are several potential sources of uncertainty in estimating the K_Ds that could not be quantified (*18*). There is also a range of K_Ds even for those chondrules that lie close to the 1:1 line. Some of this variation could be due to the gain or loss of Na after crystallization (*18*). Despite these concerns, because most chondrules fall close to the 1:1 line, we infer that to first order they were essentially closed systems for Na during crystallization.

There is some uncertainty about the nebular conditions during chondrule formation. To estimate the range of solids densities that would have been necessary for roughly closed-system behavior of Na at liquidus temperatures, we calculated the equilibrium vapor pressures over the bulk chondrule silicate melts alone as well as over the silicate melts in equilibrium with pure Fe metal (*18*). The solids densities were estimated by calculating, for a given temperature and equilibrium pressure of Na (P_{Na}), the density of solids required for 90% of the Na to remain condensed (Table 1). If the P_{H_2} was $>10^{-7}$ bars during chondrule formation, it will increase the lower limits on the densities (*18*).

The ranges of solids densities in Table 1 are much higher than previously considered for chondrule formation. In principle, the required solids densities could be lowered if the oxygen fugacity (f_{O_2}) were enhanced. However, the f_{O_2} levels in the calculations of the lower limits were well above the iron-wüstite buffer and, therefore, almost certainly already too high because chondrules contain metal. The apparent absence of chondrules exhibiting clear evidence for the open-system behavior of Na or isotopic evidence for evaporation indicates that the chondrules in chondrites formed almost exclusively in such high-density regions. Either there was a remarkably efficient process for concentrating chondrule precursors in regions with high solids densities, or only chondrules that formed in high-density regions accreted into chondrites.

On the basis of the lack of isotopic fractionations in chondrules, it has been estimated that chondrule-forming regions were at least 150 to 6000 km in radius (*24*). At the minimum liquidus densities we calculated (typically >10 g/m^3), regions >4000 km in radius will be self-gravitating (*18*). Regions of this size and density should cool at rates that are consistent with those inferred for chondrules (*18*) and contain enough mass to produce a body of the size typically assumed for the chondrite parent asteroids (radius ~50 km, density ~3 g/cc). These observations raise the possibility that planetesimal formation and chondrule formation in high-density regions were linked. In any case, such high densities would promote the aggregation of larger objects that could then coalesce into asteroid-sized objects (*25*).

A close link between chondrule and planetesimal formation would explain how distinct chondrule populations were preserved in a turbulent nebula in which large-scale mixing would have occurred relatively rapidly. At near liquidus temperatures and inferred densities, there would be gas-mediated exchange between chondrules in close proximity to one another. The diversity of chondrule compositions would thus seem to be problematic, but equilibration time scales are poorly understood and would depend on vapor pressures, diffusion rates in the melts, and the magnitude of the initial compositional differences between chondrules. Even at equilibrium, differences in bulk chondrule compositions are possible to generate simply by varying the proportions of the equilibrium phases. The finite time scales of gaseous diffusion mean that if chondrule-forming regions were relatively large, microenvironments could exist within them (*24*). However, chondrite formation cannot have immediately followed chondrule formation, because at least some chondrules experienced multiple heating events (*2*), and the low-temperature matrix that cements chondrites must also be present before final assembly (*18*).

Shock (*26*) and current-sheet (*27*) heating models both predict thermal histories that are consistent with those inferred for chondrules. The solids densities we estimate are much higher than assumed in previous models (*26*, *27*) but are more consistent with shock heating than with current sheets. Over the range of previously explored solids densities, chondrule cooling rates after shock heating are predicted to increase with increasing solids density. It remains to be seen whether the calculated cooling rates at the densities we estimate are consistent with those inferred for real chondrules. If not, other heating mechanisms, such as lightning or planetesimal collisions, will have to be explored.

References and Notes

1. R. H. Hewins, H. C. Connolly Jr., G. E. Lofgren, G. Libourel, in *Chondrites and the Protoplanetary Disk*, A. N. Krot, E. R. D. Scott, B. Reipurth, Eds. (Astronomical Society of the Pacific, San Francisco, 2005), vol. 341, pp. 286–316.
2. R. H. Jones, J. N. Grossman, A. E. Rubin, in *Chondrites and the Protoplanetary Disk*, A. N. Krot, E. R. D. Scott, B. Reipurth, Eds. (Astronomical Society of the Pacific, San Francisco, 2005), vol. 341, pp. 251–285.
3. N. T. Kita *et al.*, in *Chondrites and the Protoplanetary Disk,* A. N. Krot, E. R. D. Scott, B. Reipurth, Eds. (Astronomical Society of the Pacific, San Francisco, 2005), vol. 341, pp. 558–587.
4. J. N. Grossman, J. T. Wasson, in *Chondrules and their Origins,* E. A. King, Ed. (Lunar and Planetary Institute, Houston, TX, 1983), pp. 88–121.
5. R. H. Jones, *Geochim. Cosmochim. Acta* **54**, 1785 (1990).
6. Y. Yu, R. H. Hewins, C. M. O'D. Alexander, J. Wang, *Geochim. Cosmochim. Acta* **67**, 773 (2003).
7. J. Wang, A. M. Davis, R. N. Clayton, T. K. Mayeda, A. Hashimoto, *Geochim. Cosmochim. Acta* **65**, 479 (2001).
8. B. Cohen, R. H. Hewins, C. M. O'D. Alexander, *Geochim. Cosmochim. Acta* **68**, 1661 (2004).
9. C. M. O'D. Alexander, S. Taylor, J. S. Delaney, P. Ma, G. F. Herzog, *Geochim. Cosmochim. Acta* **66**, 173 (2002).
10. S. Taylor *et al.*, *Geochim. Cosmochim. Acta* **69**, 2647 (2005).
11. D. S. Ebel, L. Grossman, *Geochim. Cosmochim. Acta* **64**, 339 (2000).
12. C. M. O'D. Alexander, *Geochim. Cosmochim. Acta* **68**, 3943 (2004).
13. A. M. Davis, C. M. O'D. Alexander, H. Nagahara, F. M. Richter, in *Chondrites and the Protoplanetary Disk*, A. N. Krot, E. R. D. Scott, B. Reipurth, Eds. (Astronomical Society of the Pacific, San Francisco, 2005), vol. 341, pp. 432–455.
14. C. M. O'D. Alexander, J. N. Grossman, *Meteorit. Planet. Sci.* **40**, 541 (2005).
15. G. Libourel, A. N. Krot, l. Tissandier, *Lunar Planet. Sci.* **XXXIV**, 1558 (abstr.) (2003).
16. R. H. Jones, *Geochim. Cosmochim. Acta* **58**, 5325 (1994).
17. J. N. Cuzzi, R. C. Hogan, J. M. Paque, A. R. Dobrovolskis, *Astrophys. J.* **546**, 496 (2001).
18. Materials and methods are available as supporting material on *Science* Online.
19. R. H. Jones, G. E. Lofgren, *Meteoritics* **28**, 213 (1993).
20. H. Nagahara, *Nature* **292**, 135 (1981).
21. R. H. Jones, in *Chondrules and the Protoplanetary Disk*, R. H. Hewins, R. H. Jones, E. R. D. Scott, Eds. (Cambridge Univ. Press, Cambridge, 1996), pp. 163–172.
22. C. M. O'D. Alexander, J. N. Grossman, D. Ebel, *Lunar Planet. Sci.* **XXXVIII**, (2007).
23. M. S. Ghiorso, R. O. Sack, *Contrib. Mineral. Petrol.* **119**, 197 (1995).
24. J. N. Cuzzi, C. M. O'D. Alexander, *Nature* **441**, 483 (2006).
25. A. Johansen *et al.*, *Nature* **448**, 1022 (2007).
26. S. J. Desch, F. J. Ciesla, L. L. Hood, T. Nakamoto, in *Chondrites and the Protoplanetary Disk*, A. N. Krot, E. R. D. Scott, B. Reipurth, Eds. (Astronomical Society of the Pacific, San Francisco, 2005), vol. 341, pp. 849–872.
27. M. K. R. Joung, M.-M. Mac Low, D. S. Ebel, *Astrophys. J.* **606**, 532 (2004).

28. This paper is dedicated to the memory of Robert Hutchison. J. Nuth and an anonymous reviewer greatly improved this manuscript. C.A. was partially supported by NASA Origins of Solar Systems grant NNG06GE39G, J.G. was partially supported by NASA Cosmochemistry grant NNH05AB65I, D.E. was partially supported by NASA Cosmochemistry grant NANG06GD89G, and F.C. was funded by a Department of Terrestrial Magnetism Carnegie Institution of Washington postdoctoral fellowship.

Supporting Online Material

www.sciencemag.org/cgi/content/full/320/5883/1617/DC1
Methods
Fig. S1
Tables S1 to S5
References

15 February 2008; accepted 14 May 2008
10.1126/science.1156561